Effect of nanostructuring on the interaction of CO_2 with molybdenum carbide nanoparticles

Carlos Jimenez-Orozco,*[a] Marc Figueras,[b] Elizabeth Flórez,[a] Francesc Viñes,*[b]
José A. Rodriguez,[c] Francesc Illas[b]

[a] *Universidad de Medellín, Facultad de Ciencias Básicas, Grupo de Materiales con Impacto (Mat&mpac), Carrera 87 No 30-65, Medellín, Colombia*
[b] *Universitat de Barcelona, Departament de Ciència de Materials i Química Física & Institut de Química Teòrica i Computacional (IQTCUB), c/ Martí i Franquès 1-11, 08028 Barcelona, Spain.*
[c] *Brookhaven National Laboratory, Chemistry Division, Upton, New York 11973, United States of America*

Index of Contents

Table S1. Test calculations ensuring convergence of CO_2 E_{ads} with respect to vacuum region extent for Mo_4C_6 and $Mo_{32}C_{32}$ models. Only the adsorption site displaying the largest E_{ads} has been considered. ZPE is not included.

Nanoparticle	Vacuum (Å)	E_{ads} (eV)
Mo_4C_6	10.0	-1.70
	12.5	-1.70
	15.0	-1.70
	17.5	-1.69
	20.0	-1.69
$Mo_{32}C_{32}$	10.0	-2.01
	12.5	-2.00
	15.0	-2.00
	17.5	-2.00
	20.0	-2.00

Table S2. Structural isomers of the S_{set} nanoparticles predicted from the global minima search method used in this work. Relative energies (ΔE_{rel}) to the most stable isomer for each nanoparticle are listed. All values are given in eV. The [a] superindex denotes the most stable isomer as predicted by the cascade algorithm (see discussion in the main text).

Nanoparticle	Isomer	ΔE_{rel}
Mo_4C_6	1	0.00
	2	1.05
	3	1.49
	4	1.50[a]
	5	1.56
	6	1.67
	7	1.71
	8	2.25
	9	2.51
	10	2.52
	11	2.53
	12	2.55
	13	3.24
	14	4.87
	15	5.89
Mo_5C_6	1	0.00
	2	0.02
	3	0.07[a]
	4	0.09
	5	0.28
	6	0.52
	7	0.79
	8	0.91
	9	1.01
	10	2.93
Mo_6C_4	1	0.000
	2	0.15
	3	0.54[a]

	4	0.63
	5	0.69
	6	0.97
	7	1.37
	8	1.67
	9	1.81
	10	2.14
	11	3.00
	12	3.61
Mo_6C_5	1	0.00
	2	0.26[a]
	3	0.49
	4	0.60
	5	1.17
	6	1.30
	7	1.45
	8	2.06
	9	2.17
	10	3.60
Mo_6C_6	1	0.00[a]
	2	1.50
	3	1.73
	4	2.05
	5	2.62
	6	3.17
	7	3.60
	8	3.61
	9	3.81
	10	3.86
	11	4.93

Table S3. Number of initial, #Ini, and different final, #Fin, CO_2 bonding modes for each studied nanoparticle, together with the percentage, %diff, of different final geometries gained for each case; for instance, for Mo_5C_6 isomer #1, the seventy-two initial geometries led to eleven different final geometries, representing a 15% of the initial geometries.

Nanoparticle	Isomer	#Ini	#Fin	%diff
Mo_4C_6	1	5	5	100
	2	9	5	56
	3	5	5	100
	4[a]	32	22	69
	5	20	9	45
Mo_5C_6	1	72	11	15
	2	28	18	64
	3[b]	11	7	64
	4	21	7	33
Mo_6C_4	1	61	15	25
	2	55	9	16
	3[b]	24	18	75
	4	54	14	26
	5	56	11	20
Mo_6C_5	1	46	30	65
	2[b]	20	6	30
Mo_6C_6	1	22	17	77
Mo_8C_{12}	1	15	11	73
$Mo_{10}C_{12}$	1	36	21	58
$Mo_{12}C_6$	1	93	65	70
$Mo_{12}C_8$	1	125	58	46
$Mo_{12}C_{10}$	1	130	64	49
$Mo_{12}C_{12}$	1	47	37	79
$Mo_{14}C_{13}$	1	18	10	56
$Mo_{24}C_{24}$	1	45	38	84
$Mo_{32}C_{32}$	1	36	25	69

[a] Mo_4C_6 isomers not considered for further characterization.
[b] Belongs to the nanoparticle obtained *via* cascade procedure in Ref. 1

Table S4. Most stable adsorption conformation, energy quantities, and Bader charges, Q, in *e*, for the adsorbed CO_2. E_{ads}, E_{def}, E_{dist}, and E_{att} stand for the adsorption energy, the nanoparticle distortion energy, CO_2 deformation energy, and attachment energy, respectively, all given in eV. Mo/C corresponds to the atomic ratio. Results for the extended surfaces in the bottom rows, reproduced from previous work —*cf.* Refs. 2 and 3— are included for comparison.

System	Isomer	Bonding mode	E_{ads}	E_{dist}	E_{def}	E_{att}	Q	Mo/C
Mo_4C_6	1	η^2-CO_2-μ^2-C_CO_M	-1.74	0.20	2.82	-4.76	-0.57	0.67
	2	η^3-CO_2-μ^2-$C_BO_MO_M$	-2.38	0.18	1.67	-4.23	-0.80	
	3	η^2-CO_2-μ^2-C_CO_M	-3.10	0.00	2.98	-6.08	-0.65	
	4	η^3-CO_2-μ^2-$C_BO_MO_M$	-1.95	0.23	1.65	-3.83	-1.05	
	5	η^3-CO_2-μ^2-$C_BO_MO_M$	-2.61	0.07	2.15	-4.83	-0.93	
Mo_5C_6	1	η^3-CO_2-μ^2-$C_BO_MO_M$	-2.34	0.39	1.67	-4.40	-0.93	0.83
	2	η^3-CO_2-μ^2-$C_BO_MO_M$	-2.65	0.19	1.86	-4.70	-0.97	
	3	η^2-CO_2-μ^2-C_CO_M	-1.73	0.44	3.12	-5.29	-0.71	
	4	η^3-CO_2-μ^2-$C_BO_MO_M$	-2.28	0.39	3.12	-5.29	-0.71	
Mo_6C_4	1	η^3-CO_2-μ^2-$C_BO_MO_M$	-2.23	0.13	1.77	-4.13	-0.90	1.50
	2	η^3-CO_2-μ^2-$C_BO_MO_M$	-2.61	0.39	1.86	-4.86	-0.95	
	3	η^3-CO_2-μ^2-$C_BO_MO_M$	-3.18	0.08	1.86	-5.12	-1.04	
	4	η^3-CO_2-μ^2-$C_BO_MO_M$	-2.79	0.35	2.09	-5.03	-0.77	
	5	η^3-CO_2-μ^2-$C_BO_MO_M$	-2.57	0.00	1.91	-4.48	-1.00	
Mo_6C_5	1	η^3-CO_2-μ^2-$C_BO_MO_M$	-2.68	0.07	1.70	-4.45	-0.94	1.20
	2	η^2-CO_2-μ^3-C_BO_B	-2.67	0.35	3.50	-6.52	-1.25	
Mo_6C_6	1	η^2-CO_2-μ^2-C_CO_M	-1.44	0.61	2.99	-5.04	-0.70	1.00
Mo_8C_{12}		η^2-CO_2-μ^1-C_MO_M	-1.03	0.22	1.96	-3.21	-0.53	0.67
$Mo_{10}C_{12}$	1	η^3-CO_2-μ^3-$C_CO_MO_M$	-1.73	0.14	2.38	-4.25	-0.58	0.83
$Mo_{12}C_6$	1	η^3-CO_2-μ^3-$C_{HW}O_MO_M$	-2.56	0.68	3.41	-6.65	-1.35	2.00
$Mo_{12}C_8$	1	η^3-CO_2-μ^3-$C_{HW}O_MO_M$	-2.44	0.40	4.26	-7.10	-1.28	1.50
$Mo_{12}C_{10}$	1	η^3-CO_2-μ^3-$C_{HW}O_MO_M$	-2.03	0.60	4.10	-6.73	-1.42	1.20
$Mo_{12}C_{12}$	1	η^2-CO_2-μ^2-C_CO_M	-1.53	0.65	2.95	-5.13	-0.58	1.00
$Mo_{14}C_{13}$		η^3-CO_2-μ^3-$C_CO_MO_M$	-1.45	0.26	2.26	-3.97	-0.73	1.08
$Mo_{24}C_{24}$		η^2-CO_2-μ^2-C_CO_M	-2.14	0.37	3.48	-5.99	-0.42	1.00
$Mo_{32}C_{32}$		η^3-CO_2-μ^3-$C_BO_MO_M$	-1.97	0.93	3.50	-6.40	-0.61	1.00
δ-MoC(001)		η^1-CO_2-μ^1-C_C	-1.20	0.16	2.48	-3.84	-0.62	1.00
β-Mo_2C(001)-C		η^2-CO_2-μ^2-C_CO_M	-1.32	0.53	2.83	-4.68	-0.56	2.00
β-Mo_2C(001)-Mo		η^3-CO_2-μ^3-$C_BO_MO_B$	-1.87	0.15	3.12	-5.14	-0.87	2.00

Fig. S1. Geometry of most stable isomers of the considered nanoparticles in the S_{set}. Mo and C atoms are shown as magenta and brown spheres, respectively.

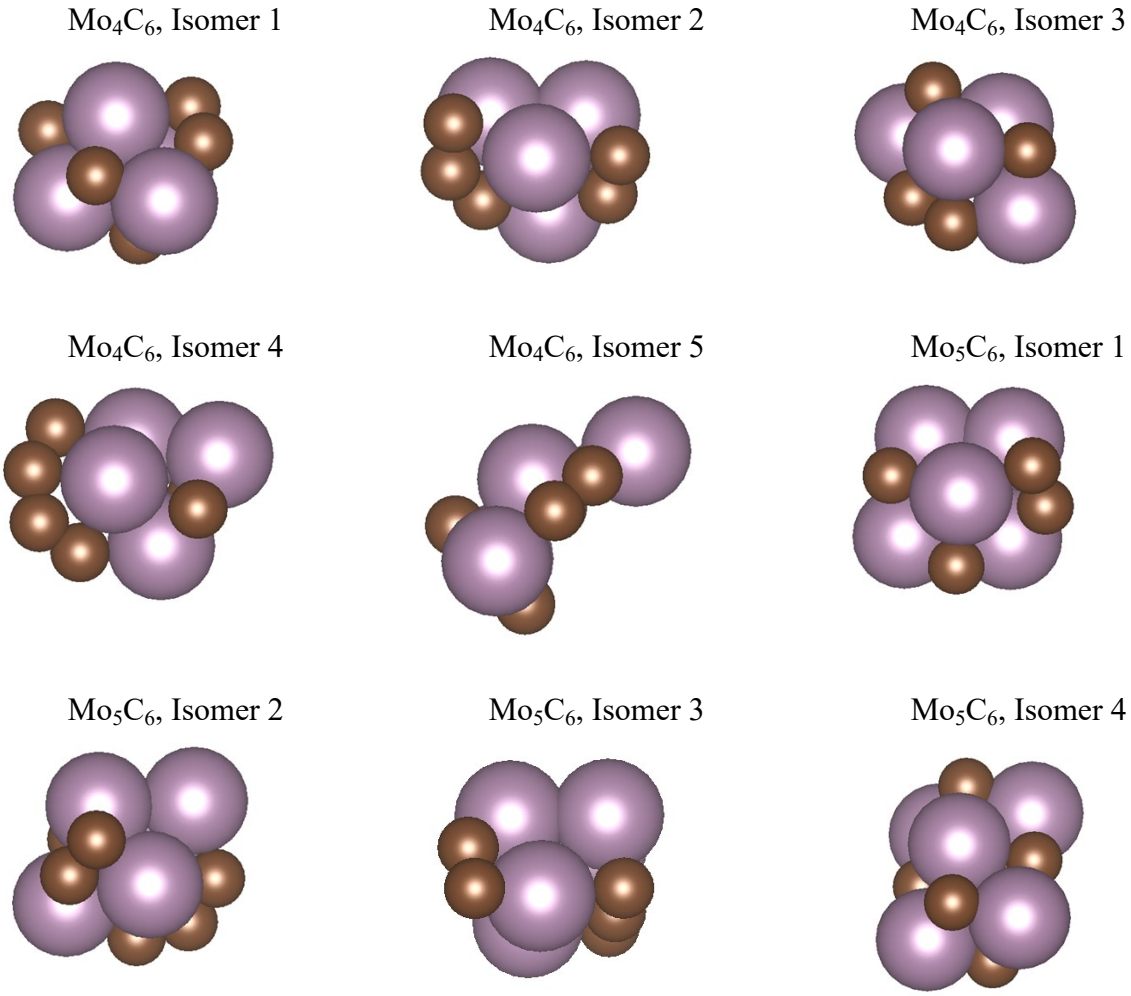

Mo_6C_4, Isomer 1

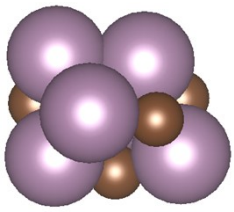

Mo_6C_4, Isomer 2

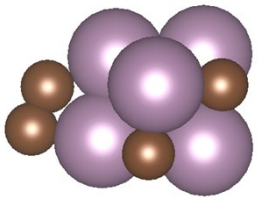

Mo_6C_4, Isomer 3

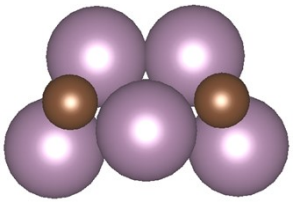

Mo_6C_4, Isomer 4

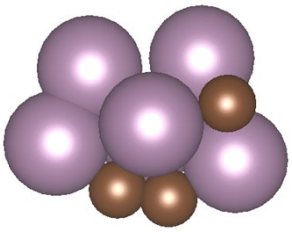

Mo_6C_4, Isomer 5

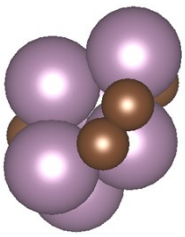

Mo_6C_5, Isomer 1

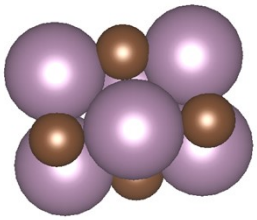

Mo_6C_5, Isomer 2

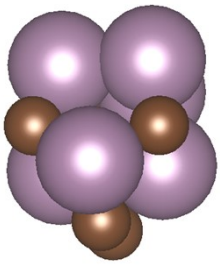

Mo_6C_6, Isomer 1

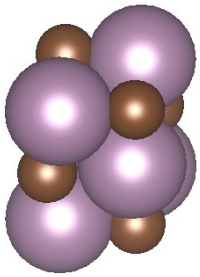

Fig. S2. Most stable structure and adsorption energy for CO_2 interacting with $Mo_{12}C_{12}$, $Mo_{24}C_{24}$, and $Mo_{32}C_{32}$ nanoparticles on vertex (top images), facet (middle images), and lateral (bottom images) modes. Colors as in Fig. S1, but CO_2 C and O atoms are shown as black and red spheres. Adsorption site labeling and E_{ads} values are also provided.

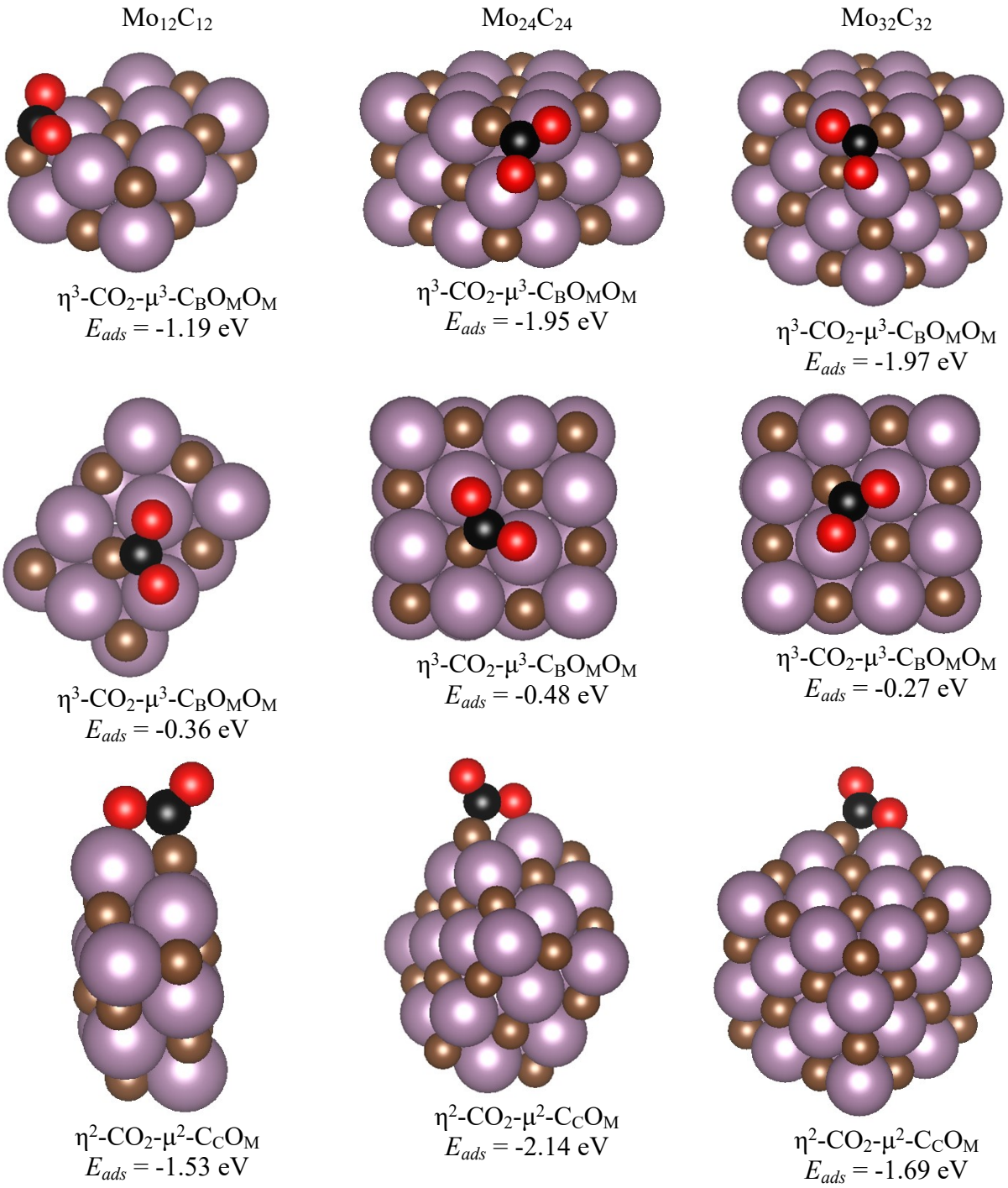

Fig. S3. Top (top images) and side (bottom images) views for CO_2 adsorption on extended surfaces δ-MoC (001) (left), β-Mo_2C(001)-C (middle), and β-Mo_2C(001)-Mo, reproduced from Refs. 2 and 3, and included for comparison. Colors as in Figs. S1 and S2. Adsorption modes and energies are included.

η^1-CO_2-μ^1-C_C	η^2-CO_2-μ^2-C_CO_M	η^3-CO_2-μ^3-$C_BO_MO_B$
E_{ads} = -1.20 eV	E_{ads} = -1.32 eV	E_{ads} = -1.87 eV

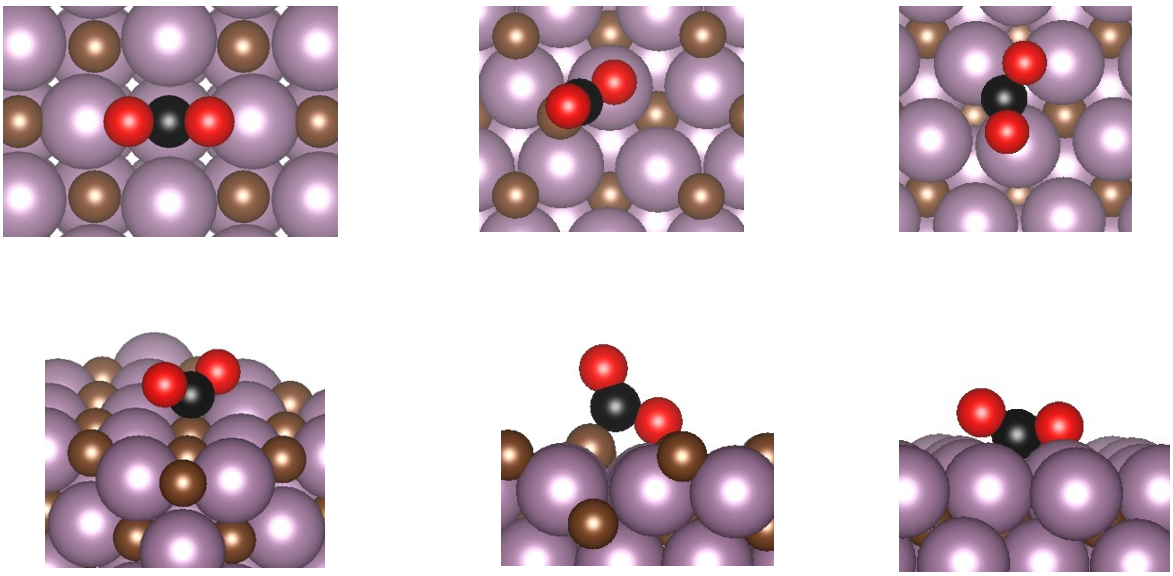

Fig. S4. CO_2 adsorption on small Mo_4C_6, Mo_5C_6, Mo_6C_4, Mo_6C_5, and Mo_6C_6 clusters, and intermediate Mo_8C_{12}, $Mo_{10}C_{12}$, $Mo_{12}C_6$, $Mo_{12}C_8$, $Mo_{12}C_{10}$, and $Mo_{14}C_{13}$ nanoparticles. Color code as in Fig. S3.

Mo_4C_6, Isomer 1

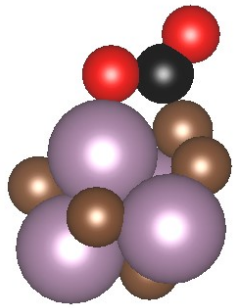

Mo_4C_6, Isomer 2

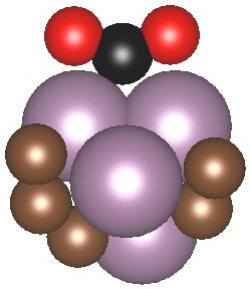

Mo_4C_6, Isomer 3

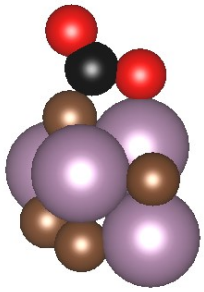

Mo_4C_6, Isomer 4

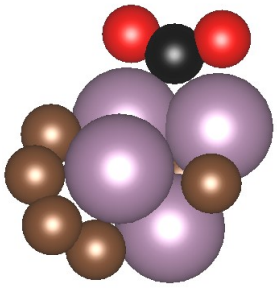

Mo_4C_6, Isomer 5

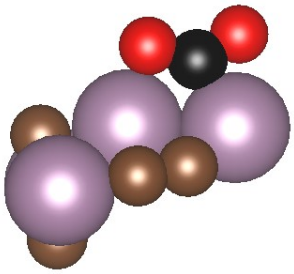

Mo_5C_6, Isomer 1

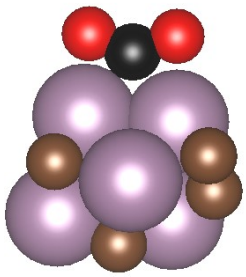

Mo_5C_6, Isomer 2

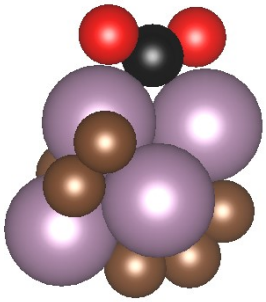

Mo_5C_6, Isomer 3

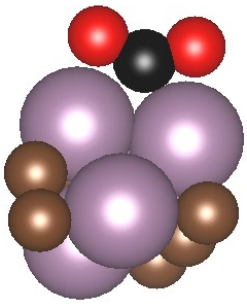

Mo_5C_6, Isomer 4

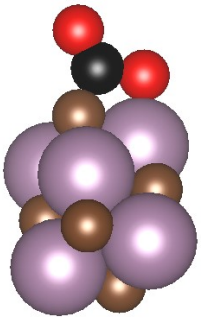

Mo_6C_4, Isomer 1

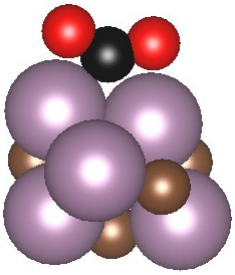

Mo_6C_4, Isomer 2

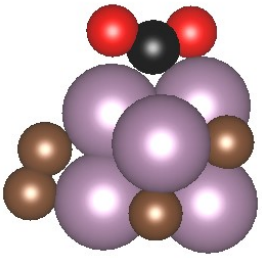

Mo_6C_4, Isomer 3

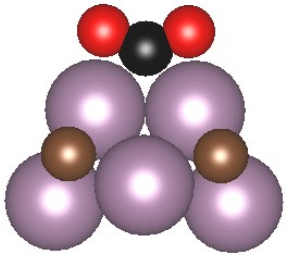

Mo_6C_4, Isomer 4

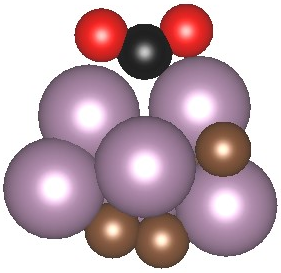

Mo_6C_4, Isomer 5

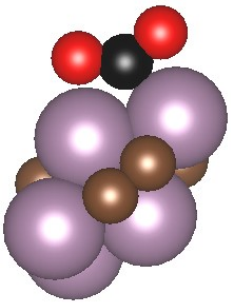

Mo_6C_5, Isomer 1

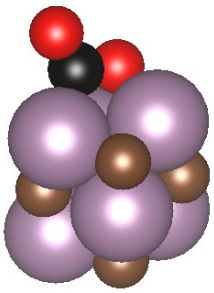

Mo_6C_5, Isomer 2

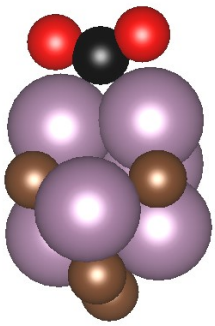

Mo_6C_6, Isomer 1

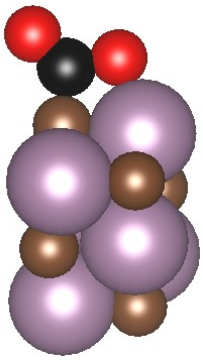

Mo_8C_{12} (MetCar)

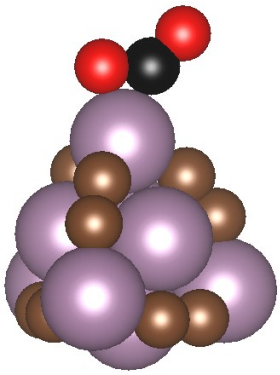

$Mo_{10}C_{12}$

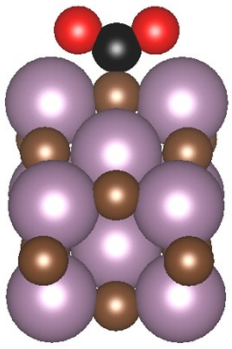

$Mo_{12}C_6$

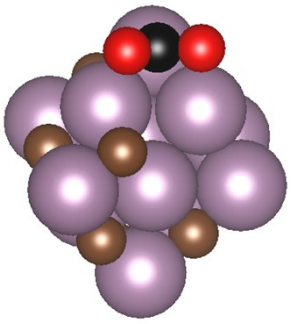

$Mo_{12}C_8$

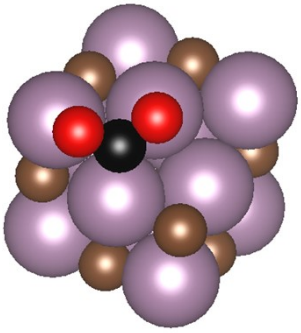

$Mo_{12}C_{10}$

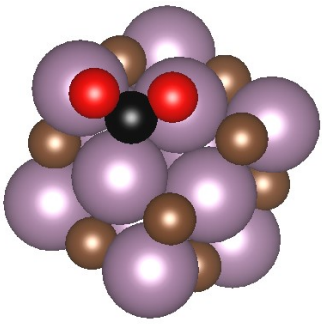

$Mo_{14}C_{13}$ (nanocube)

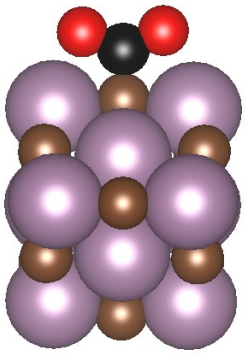

Fig. S5. Evolution of the attachment energy, E_{att}, in eV, and Bader charges, Q, in *e*, for CO_2 adsorbed on small nanoparticles *via* η^3-CO_2-μ^2-$C_BO_MO_M$ mode, as a function of the Mo/C ratio.

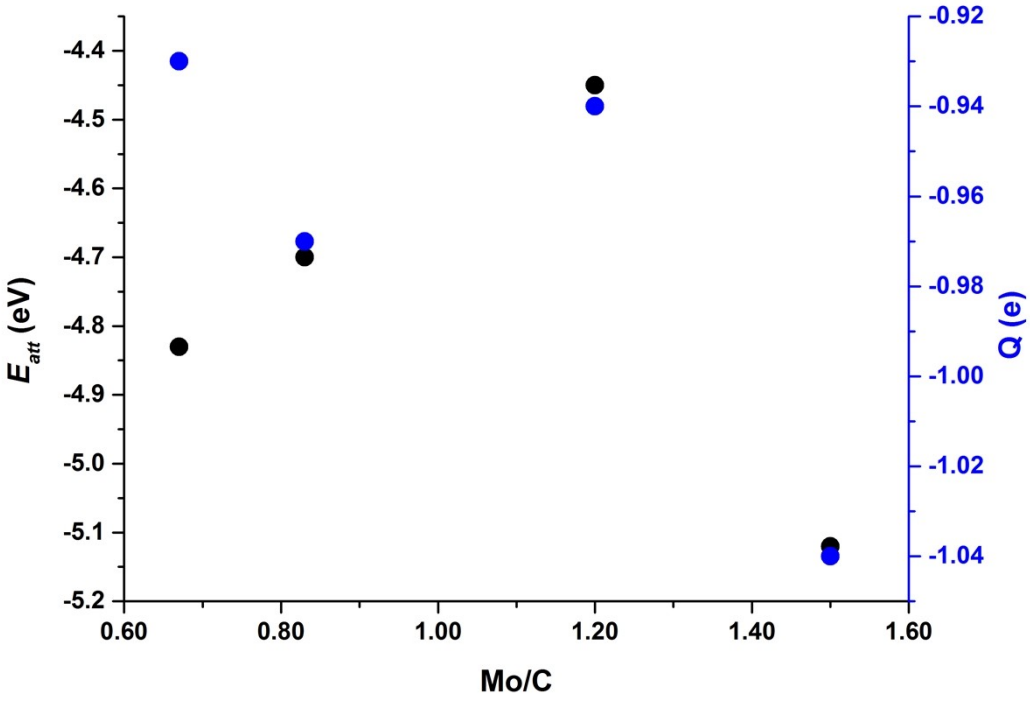

Fig. S6. CO_2 deformation energy, E_{def}, in eV, and Bader charge, Q, in *e*, for CO_2 adsorbed on the nanoparticles in S_{set} as a function of the Mo/C ratio, considering in each case the most stable structure, regardless of the bonding mode. Note that this is different from Fig. S5 where only the η^3-CO_2-μ^2-$C_BO_MO_M$ bonding mode was always considered.

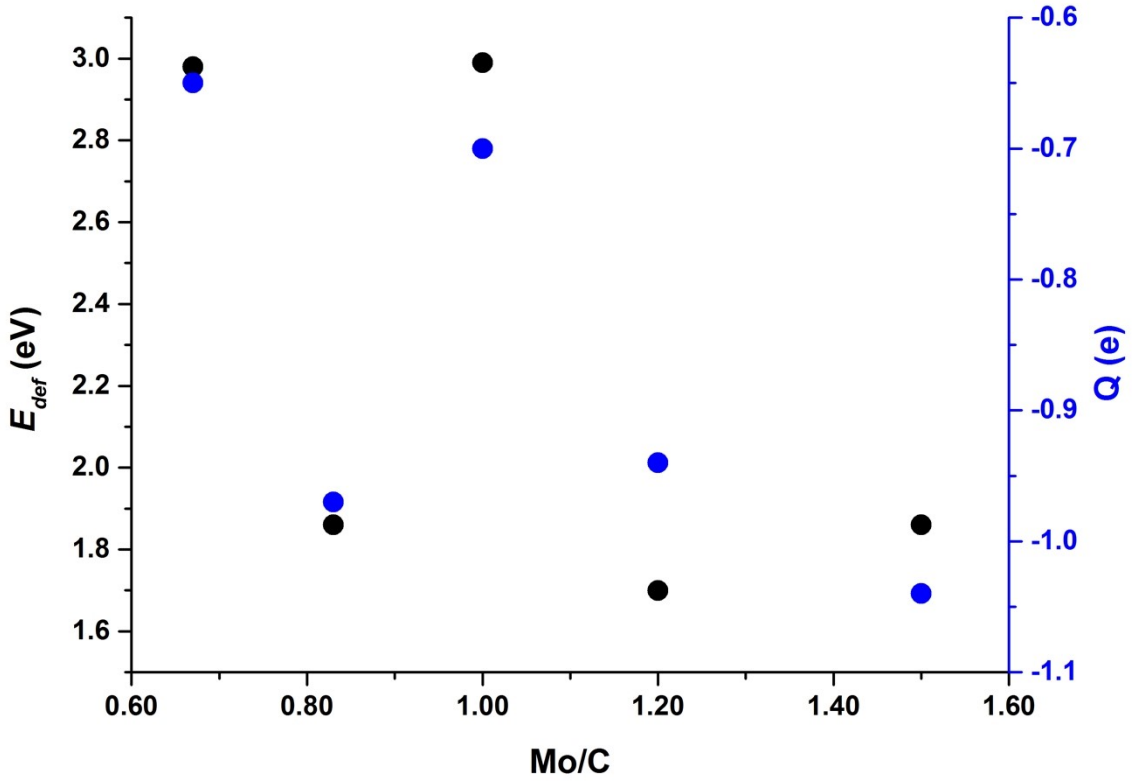

Fig. S7. CO_2 attachment energy, E_{att}, in eV, and Bader charges, Q, in *e*, on the adsorbed molecule for the most stable CO_2 bonding mode on the different nanoparticles.

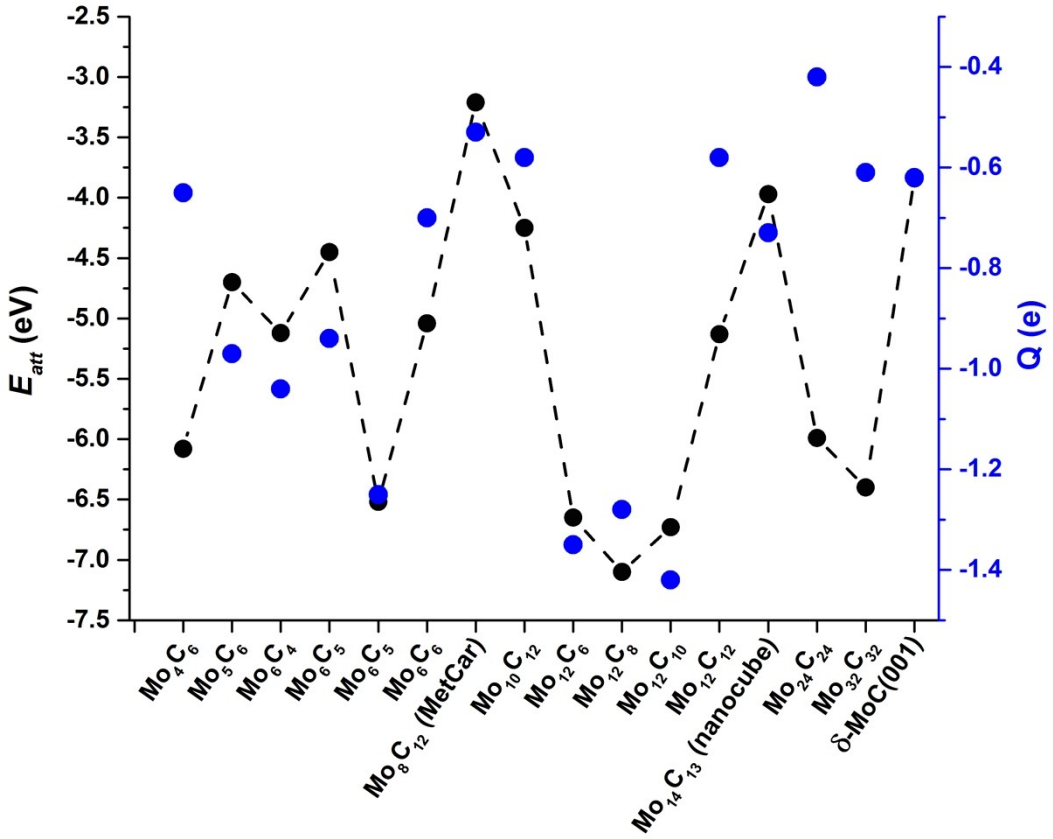

References

1 C. Jimenez-Orozco, M. Figueras, E. Flórez, F. Viñes, J. A. Rodriguez and F. Illas, *J. Phys. Chem. C*, 2021, **125**, 6287–6297.

2 S. Posada-Pérez, F. Viñes, P. J. Ramirez, A. B. Vidal, J. A. Rodriguez and F. Illas, *Phys. Chem. Chem. Phys.*, 2014, **16**, 14912-14921.

3 M. Figueras, A. Jurado, A. Morales-García, F. Viñes, and F. Illas, *Phys. Chem. Chem. Phys.*, 2020, **22**, 19249-19253.